HOKKAIDO UNIVERSITY

Title	Seasonal and Inter-Annual Variations in pCO2sea and Air-Sea CO2 Fluxes in Mid-Latitudes of the Western and Eastern North Pacific during 1999-2006 : Recent Results Utilizing Voluntary Observation Ships
Author(s)	Takamura, Tomomi Ryu; Inoue, Hisayuki Yoshikawa; Midorikawa, Takashi et al.
Citation	Journal of the Meteorological Society of Japan, 88(6), 883-898 https://doi.org/10.2151/jmsj.2010-602
Issue Date	2010-12
Doc URL	https://hdl.handle.net/2115/46939
Type	journal article
File Information	JMSJ88-6_883-898.pdf

Hokkaido University Collection of Scholarly and Academic Papers : HUSCAP

Journal of the Meteorological Society of Japan, Vol. 88, No. 6, pp. 883–898, 2010.
DOI:10.2151/jmsj.2010-602

Seasonal and Inter-Annual Variations in pCO_2^{sea} and Air-Sea CO_2 Fluxes in Mid-Latitudes of the Western and Eastern North Pacific during 1999–2006: Recent Results Utilizing Voluntary Observation Ships

Tomomi Ryu TAKAMURA, Hisayuki Yoshikawa INOUE

Graduate School of Environmental Science, Hokkaido University, Sapporo, Japan

Takashi MIDORIKAWA, Masao ISHII

Geochemical Research Department, Meteorological Research Institute, Tsukuba, Japan

and

Yukihiro NOJIRI

Climate Change Research Project, National Institute for Environmental Studies, Tsukuba, Japan

(Manuscript received 19 November 2009, in final form 28 August 2010)

Abstract

We have investigated the seasonal and inter-annual variations of the difference in partial pressure of CO_2 between surface seawater (pCO_2^{sea}) and overlying air (pCO_2^{air}) and the air-sea CO_2 flux in the mid-latitudes of the western North Pacific (WNP; 25–40°N, 140–170°E) and eastern North Pacific (ENP; 25–40°N, 120–150°W) from 1999 to 2006 using the latest voluntary observation ship data. In the WNP and ENP, the area-averaged ΔpCO_2 ($pCO_2^{air} - pCO_2^{sea}$) was at its minimum in late summer (−4.6 to 6.7 μatm in the WNP and −32.5 to −20.5 μatm in the ENP) and at its maximum in late winter (51.0 to 59.8 μatm in the WNP and 35.1 to 46.2 μatm in the ENP). The WNP acts as a moderate sink for atmospheric CO_2 (4.1 to 5.5 mmol m^{-2} d^{-1}), while the ENP acts as a weak sink (1.1 to 1.9 mmol m^{-2} d^{-1}). Because ΔpCO_2 is mainly controlled by pCO_2^{sea}, we have evaluated the effect of the factors controlling pCO_2^{sea}: sea surface temperature (SST), salinity (SSS), dissolved inorganic carbon (TCO_2), and total alkalinity (A_T). In the WNP, not only SST but also TCO_2 plays an important role in the seasonal pCO_2^{sea} variation, while the SST could only explain most of the pCO_2^{sea} variation in the ENP. From 1999 to 2006, pCO_2^{sea} increased at a significantly lower rate (0.53 ± 0.11 μatm yr^{-1}) than pCO_2^{air} (1.81 ± 0.01 μatm yr^{-1}) in the WNP, and at a slightly lower rate in the ENP (1.32 ± 0.16 μatm yr^{-1}). The air-sea CO_2 flux increased at a rate of 0.19 ± 0.05 mmol m^{-2} d^{-1} yr^{-1} in the WNP and 0.09 ± 0.03 mmol m^{-2} d^{-1} yr^{-1} in the ENP, suggesting that the WNP is a stronger sink for atmospheric CO_2.

1. Introduction

The subtropical gyre occupies most of the mid-latitude North Pacific. In the western North Pacific subtropical gyre, the Kuroshio, known as a western boundary current, and the Kuroshio extension carry relatively warm and salty water from the south. Subtropical mode water is formed south of

Corresponding author: Tomomi Ryu Takamura, Graduate School of Environmental Science, Hokkaido University, N10W5, Kita-ku, Sapporo, Hokkaido 060-0810, Japan.
E-mail: takamura@ees.hokudai.ac.jp
© 2010, Meteorological Society of Japan

the Kuroshio extension front by significant deepening of the mixed layer in winter (Suga and Hanawa 1990). The formation and transport of mode water play an important role in the uptake of anthropogenic CO_2 (Sabine *et al.* 2004; Rodgers *et al.* 2008). The Oyashio-Kuroshio transition region lies to the north of the Kuroshio front, and is influenced by both the Kuroshio and the Oyashio (a part of the subarctic gyre that has cold and fresh water). There are numerous eddies and thermohaline fronts which are irregularly distributed (Kawai 1972). In the eastern North Pacific subtropical gyre, the California current, affected by cold and fresh subarctic water, flows southward. Along the shore of North America, the coastal upwelling enhances biological production due to the supply of nutrients from subsurface layers to the upper layer (Wooster and Reid 1963).

By compiling the partial pressure of CO_2 in surface seawater (pCO_2^{sea}) data observed since the 1970s, Takahashi *et al.* (2009) reported that the western North Pacific (WNP) is the area where the largest air-sea CO_2 flux (oceanic CO_2 uptake) occurred in the Pacific Ocean, while the eastern North Pacific (ENP) is a weak sink for atmospheric CO_2. In the Kuroshio extension, Ogawa *et al.* (2006) confirmed a large air-sea CO_2 flux in 1999 and 2000 using voluntary observation ship (VOS) pCO_2^{sea} data. Inoue *et al.* (1995) and Midorikawa *et al.* (2006) reported large effects of SST and biological activity on the seasonal variation in pCO_2^{sea}, and an increases in pCO_2^{sea} parallel to that of air in the western North Pacific (137°E). In the subarctic North Pacific, Zeng *et al.* (2002) compared the pCO_2^{sea} results with those of Takahashi *et al.* (1997), and Chierici *et al.* (2006) reported large spatial and seasonal variability of pCO_2^{sea} and air-sea CO_2 flux using VOS pCO_2^{sea} data. In the area including the Kuroshio extension (30°N–40°N, 150°E–180°E), Takahashi *et al.* (2006) reported low decadal rates of change in pCO_2^{sea} (7–9 μatm decade^{-1}). At the same latitudes of the eastern North Pacific, they reported a wide decadal rate of change in pCO_2^{sea} (2–17 μatm decade^{-1}). Using an ocean model, Rodgers *et al.* (2008) discussed the decadal increases in the seasonal cycle of ΔpCO_2 (pCO_2^{air}-pCO_2^{sea}), which are associated with changes in the large-scale circulation of the North Pacific. While pCO_2^{sea} and the carbonate system along 137°E have been examined rather extensively (see, for example, Inoue *et al.* 1995; Ishii *et al.* 2001; Midorikawa *et al.* 2003, 2006), details of pCO_2^{sea} in the WNP (especially in the Kuroshio extension) and ENP have not been reported. For clarification of the variations in pCO_2^{sea}, the CO_2 flux and its controlling factors in the wide area of the WNP and ENP are of particular importance for determining how and to what extent the air-sea CO_2 flux is changing.

In this work, we examined the seasonal/inter-annual variations in pCO_2^{sea} and air-sea CO_2 flux in the mid-latitudes of the western and eastern North Pacific using pCO_2^{sea} and pCO_2^{air} data measured from 1999 to 2006. In order to elucidate temporal variations in pCO_2^{sea} and the air-sea CO_2 flux, we used a multiple linear relationship that included the sea surface temperature (SST), sea surface salinity (SSS), and time which adequately fits the pCO_2^{sea} data taken in the WNP and ENP.

2. Data and methods

Oceanic and atmospheric CO_2 measurements, along with SST and SSS measurements, were made quasi-continuously onboard the voluntary observation ships M/S *Alligator Liberty* (Mitsui O.S.K. Lines, Ltd.) and M/S *Pyxis* (Toyofuji Shipping Co., Ltd.). For the measurement details, refer to Ogawa *et al.* (2006) and Chierici *et al.* (2006).

Nine crossings were operated by M/S *Alligator Liberty* between Tokyo, Japan, and Manzanilo, Republic of Panama, from January 1999 to October 2000. M/S *Pyxis* has two major sailing routes: one from Toyohashi, Japan to Portland, Oakland, and Long Beach, USA, and the other to the East Coast of the USA via the Panama Canal. For our analysis, we used pCO_2^{sea} data obtained during 62 crossings from July 2002 to April 2006. pCO_2^{sea} data observed aboard the M/S *Alligator Liberty* and M/S *Pyxis* are available from the World Meteorological Organization/World Data Center for Greenhouse Gases (WMO WDCGG, Tokyo, Japan, http://gaw.kishou.go.jp/wdcgg/) and Carbon Dioxide Analysis Center (CDIAC, Oak Ridge, USA, http://cdiac.ornl.gov/oceans/), respectively.

We determined the area of the WNP as 25°N–40°N, 140°E–170°E (5.0×10^6 km^2) and that of the ENP as 25°N–40°N, 120°W–150°W (4.4×10^6 km^2), by taking into account the frequency of observation and the physical/chemical properties of the water (Fig. 1). Because of a lack of data south of 30°N in the WNP, data acquired aboard the R/V *Ryofu Maru* (Japan Meteorological Agency) during the period from 1999 to 2006 were

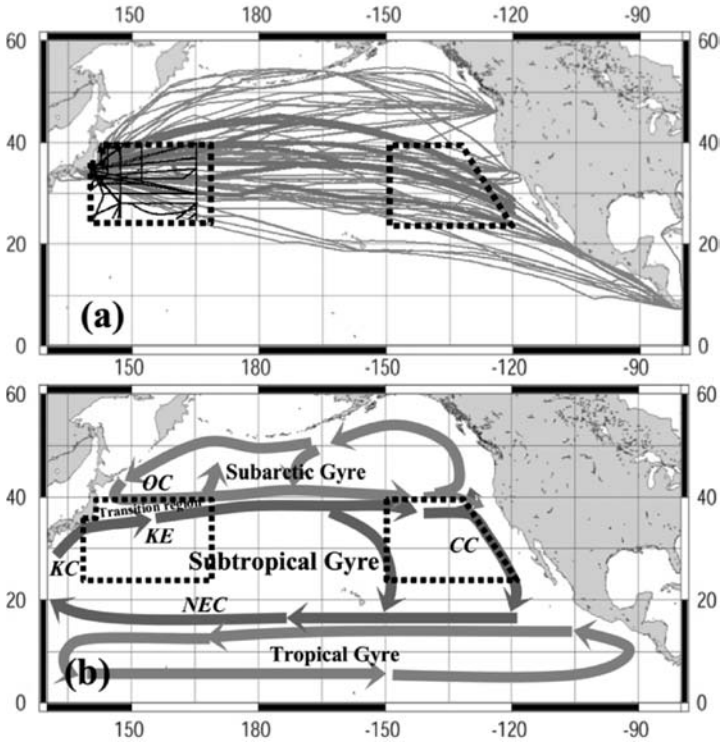


Fig. 1. Map of the study area in the North Pacific. The area surrounded by the black dotted line in each panel shows the WNP and ENP. (a) Cruise tracks of the M/S *Alligator Liberty* (thick gray line), M/S *Pyxis* (thin light gray line), and R/V *Ryofu Maru* (thin black line). (b) General circulation in the North Pacific. The major currents shown are: KC, Kuroshio current; KE, Kuroshio extension; OC, Oyashio current; CC, California current (http://www.data.kishou.go.jp/kaiyou/db/obs/knowledge/circulation.html).

also used (http://gaw.kishou.go.jp/wdcgg/). According to Chierici *et al.* (2006), the precision of the mole fraction of CO_2 (xCO_2) data from M/S *Pyxis* was about 0.5 ppm. The pCO_2^{sea} data obtained from M/S *Alligator Liberty* and R/V *Ryofu Maru* have an inclusive precision of less than 2–3 μatm.

The air-sea CO_2 flux (F) was calculated from the gas-transfer velocity (k_s) as a quadratic function of the wind speed at given SST and SSS (Sweeney *et al.* 2007), the solubility of CO_2 in seawater (α, Weiss 1974), and ΔpCO_2, and is given by: $F = k_s \alpha \Delta pCO_2$. We used the gas-transfer velocity given by Sweeney *et al.* (2007) because it has been reported to yield piston velocity values consistent with those obtained from some small-scale deliberate tracer studies and with the total bomb-^{14}C inventory obtained for the stratosphere and troposphere. Sweeney *et al.* (2007) found a globally averaged gas-transfer velocity for CO_2 33% lower than that found by Wanninkhof (1992), which was commonly used for air-sea CO_2 flux estimations. Using an updated wind speed, Takahashi *et al.* (2009) derived a gas-transfer velocity that is 4% lower than that given by Sweeney *et al.* (2007). We obtained the gridded data (1° by 1°) of pCO_2^{sea} in the WNP and ENP using SST and SSS fields (Section 3.1). Weekly temperature and salinity data of the NCEP Pacific Ocean Analysis (http://www.cdc.noaa.gov/cdc/data.ncep.pac.ocean.html) were used to calculate the monthly mean pCO_2^{sea} values. The monthly wind-speed data were taken from the reanalysis done by NCEP/NCAR (http://www.cdc.noaa.gov/cdc/data.ncep.reanalysis.derived.surface.html). We also calculated the values of the total alkalinity (A_T) and dissolved inorganic carbon (TCO_2) in surface waters. The A_T value was obtained using the equations given by Lee *et al.* (2006), and the TCO_2 value was obtained using pCO_2^{sea} and A_T (DOE 1994).

3. Results and discussion

3.1 Relationship between pCO_2^{sea} and SST, SSS, and time

Extrapolation schemes are advantageous for extending coverage in time and space, as discussed by Wanninkhof *et al.* (1996). Historically, pCO_2^{sea} has been expressed as a function of SST based on the assumption that, either directly or indirectly, the temperature is related to the ocean dynamics (lateral transport, vertical mixing, and upwelling), biological activities, and thermodynamics (Lee *et al.* 1998), which are the major processes controlling pCO_2^{sea} through the changes in A_T, TCO_2, pH, and a solubility coefficient and equilibrium constants. In Fig. 2, we plotted pCO_2^{sea} against SST. Plotting the positions of pCO_2^{sea} of the negative correlation on a map (Fig. 2) revealed that they existed mostly in the Oyashio-Kuroshio transition region of the WNP. Based on previous studies (Midorikawa *et al.* 2003; Chierici *et al.* 2006), it is likely that the negative correlation was caused by the supply of TCO_2-rich subsurface water (higher pCO_2^{sea} with lower temperature) through vertical mixing in winter, and through active biological production in spring through summer (lower pCO_2^{sea} with higher temperature). By contrast, pCO_2^{sea} values with a positive correlation were mostly found in the subtropics of the WNP, where the thermodynamic temperature effect is a major factor in controlling pCO_2^{sea} variations (Weiss *et al.* 1982; Tans *et al.* 1990; Inoue *et al.* 1995). However, the temperature effect calculated from pCO_2^{sea} and SST for temperatures above 17.5°C was 1.96%°C^{-1}, which is about a half of the thermodynamic temperature effect of 4.23%°C^{-1} (Takahashi *et al.* 1993).

The ENP is a region that has subtropical features even in northern areas as can be expected from the low surface chlorophyll density (Polovina *et al.* 2001) and low concentration of nutrients (Ogawa *et al.* 2006; http://www.nodc.noaa.gov/cgi-bin/OC5/WOA05F). However, in the ENP, the variation of pCO_2^{sea} is not definitely expressed by the SST (Fig. 2; Stephens *et al.* 1995; Landrum *et al.* 1996). In the ENP, the SSS varied largely when compared with in the WNP. In addition to SST, SSS could assist in the prediction of pCO_2^{sea} because salinity is also related to the ocean dynamics, dilution/condensation of TCO_2, A_T, and variations in the solubility coefficient and equilibrium constants. In both areas, a linear function of SST, SSS, and time (t), which was introduced to express temporal variation (Eq. (1)), fitted the observed data better than the pCO_2^{sea}-SST relationship (Table 1).

$$pCO_2^{sea} = a_0 + a_1 SST + a_2 SSS + a_3 t, \qquad (1)$$

in which t means the elapsed time (month) since January 1999 and a_j is a coefficient determined by the least-squares method. In the ENP, adding SSS to the equation as a variable provided the largest improvement in the overall correlation.

In Fig. 3, we plotted pCO_2^{sea} against SST and SSS to observe the SST and SSS dependences of pCO_2^{sea} in the WNP and ENP. The thermodynamic

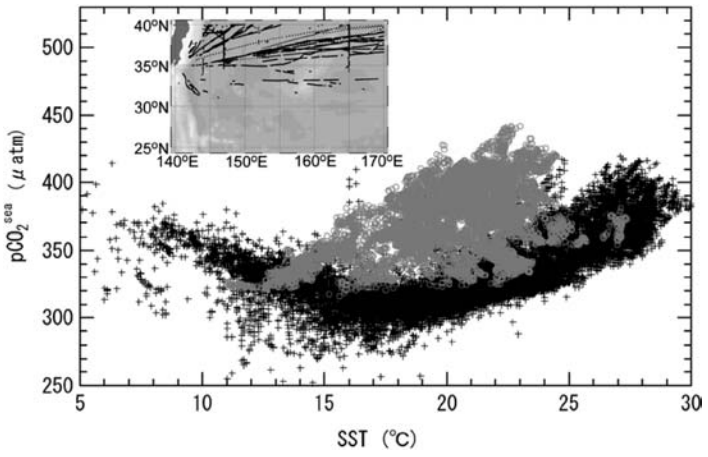


Fig. 2. Relationship between pCO_2^{sea} and SST in the WNP and ENP. The gray open circles show pCO_2^{sea} in the ENP, and the black plus symbols, represent pCO_2^{sea} in the WNP. The inset shows the positions of pCO_2^{sea} having a negative correlation with SST < 17.5°C in the WNP.

Table 1. Regression equations expressing pCO_2^{sea} as a function of SST, SSS, and t in the WNP and ENP in 1999 and 2006. Term t is the elapsed time (month) since January 1999.

	Equation	r	rms	n
WNP	$pCO_2^{sea} = -4.93SST + 0.0363t + 389.8$ (<17.5°C)	0.65	±13.8	5713
	$pCO_2^{sea} = 6.69SST + 0.0629t + 180.1$ (≥17.5°C)	0.86	±12.4	23458
	$pCO_2^{sea} = -5.62SST + 10.9SSS + 0.0071t + 26.50$ (<17.5°C)	0.68	±13.4	5713
	$pCO_2^{sea} = 6.57SST - 8.93SSS + 0.0854t + 490.7$ (≥17.5°C)	0.86	±12.1	23458
ENP	$pCO_2^{sea} = 4.60SST - 0.0939t + 286.3$	0.50	±21.9	12776
	$pCO_2^{sea} = 9.85SST - 30.7SSS - 0.0165t + 1220$	0.89	±11.3	12776

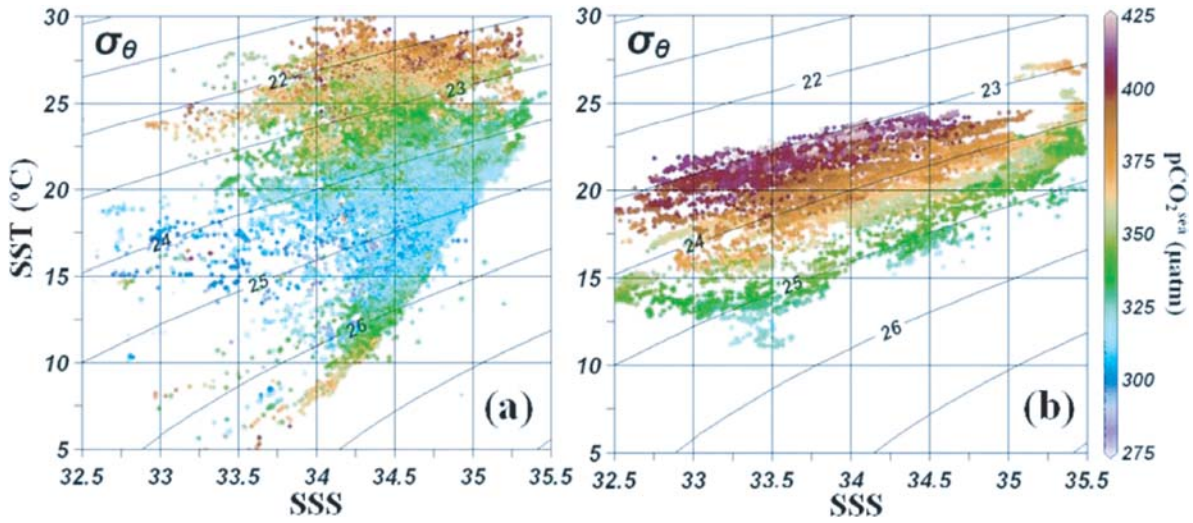


Fig. 3. SST and SSS dependences of pCO_2^{sea} in (a) the WNP and (b) the ENP. The thin lines in the panel indicate the densities calculated from SST and SSS. The numbers on the lines show σ_θ expressed as (density-1000 kg m^{-3}).

salinity effect, which includes a concentration change caused by the addition or removal of fresh water, has a positive effect on pCO_2^{sea} (Takahashi *et al.* 1993). Therefore, the negative salinity dependence of pCO_2^{sea} in the ENP suggests that the effect of the ocean dynamics is larger than that of the thermodynamic salinity effect.

Because different processes affect pCO_2^{sea} in the WNP and ENP, robust predictions of pCO_2^{sea} require sophisticated carbon cycle models, time series data, and large-scale observations. However, the simple parameterization used in this work is still useful to interpolate/extrapolate pCO_2^{sea} both spatially and temporally on the basis of the measurements underway. We examined the seasonal variations in ΔpCO_2 and air-sea CO_2 flux in the WNP and ENP, which are reconstructed from the SST and SSS fields prepared by NCEP. Because the relative contribution of the thermodynamics to the total varies seasonally (Bates *et al.* 1996; Lee *et al.* 1998), it could lead to different pCO_2^{sea}-SST, SSS relationships during the annual cycle. However, in each region, the pCO_2^{sea}-SST, SSS relationship did not vary considerably during the annual cycle within the scatter of data. Therefore, we used the linear equations listed in Table 1 to examine the average features of pCO_2^{sea} over the period from 1999 to 2006.

As mentioned so far, the WNP includes two distinguishable regions with different pCO_2^{sea}-SST, SSS relationships. Therefore, in this study, we divided the WNP at 35°N into two regions. Hereafter, north of 35°N (nWNP) is regarded as the Oyashio-Kuroshio transition region, and south of

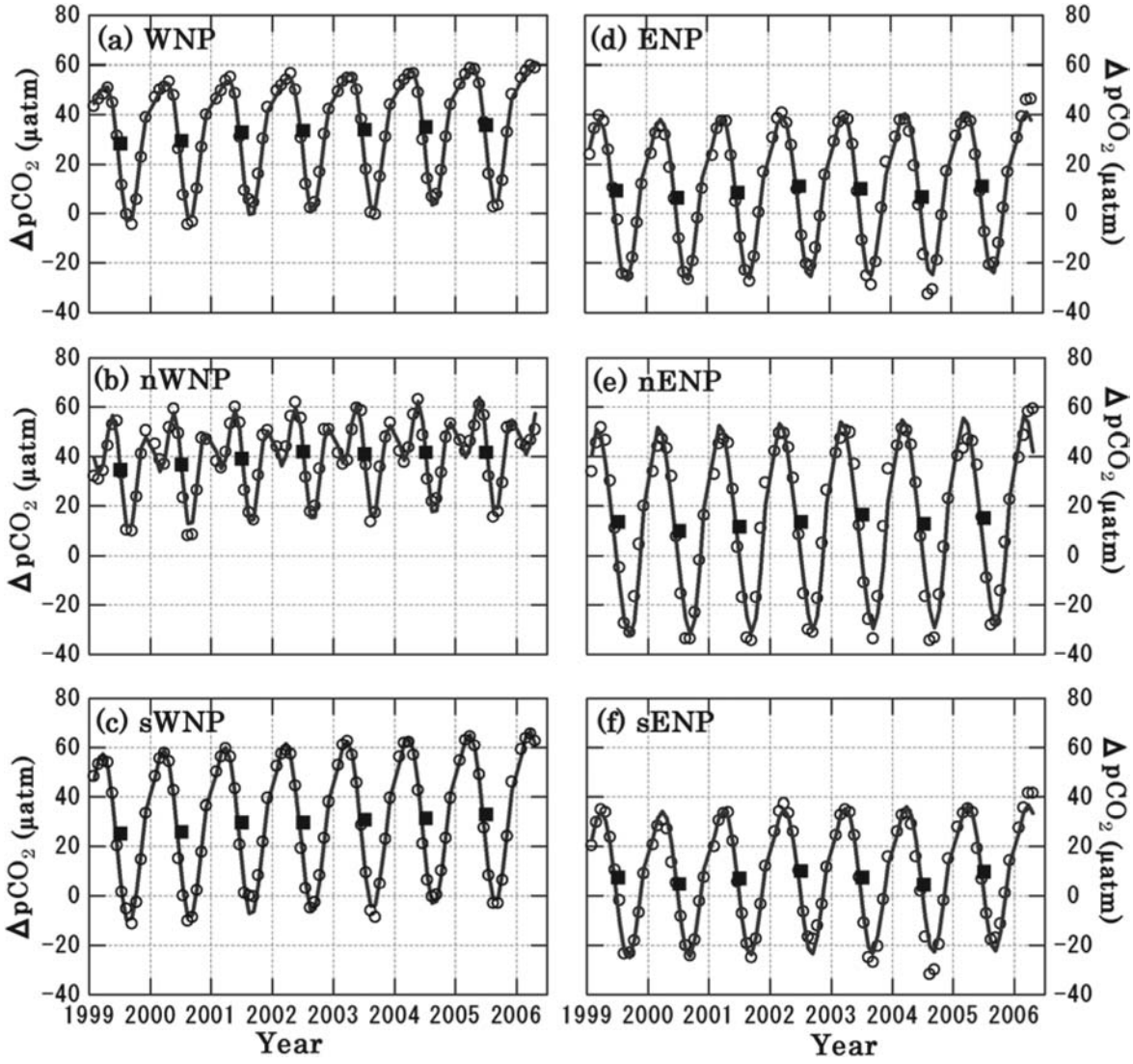


Fig. 4. Seasonal variation in ΔpCO_2 in the (a) entire WNP, (b) nENP (north of 35°N in the WNP), (c) sWNP (south of 35°N in the WNP), (d) entire ENP, (e) nENP (north of 35°N in the ENP), and (f) sENP (south of 35°N in the ENP) from 1999 to 2006. The open circles indicate the monthly ΔpCO_2, and the solid squares, represent the annual mean ΔpCO_2. The black line shows the results calculated using Eq. (2).

35°N (sWNP), as the western North Pacific Subtropical Gyre. Although the ENP shows a single pCO_2^{sea}-SST, SSS relationship, we also divided the ENP at 35°N into two regions so as to compare pCO_2^{sea} and air-sea CO_2 flux in the WNP and ENP.

3.2 Variation in ΔpCO_2

a. Seasonal variation in ΔpCO_2 and its controlling factors

Figure 4 shows the variation in ΔpCO_2 in the WNP and ENP. The observed pCO_2^{air} data were fitted to a harmonic function $f(t)$:

$$f(t) = b + \sum_{i=1}^{2}\left\{c_i \cos\left(\frac{2\pi i}{12}t\right) + d_i \sin\left(\frac{2\pi i}{12}t\right)\right\} + et \tag{2}$$

to estimate the monthly pCO_2^{air} ($f(t) = pCO_2^{air}(t)$). In Eq. (2), b, c_i, d_i, and e are constants determined by the least-squares method. After calculating the monthly ΔpCO_2, the ΔpCO_2 data were fitted to

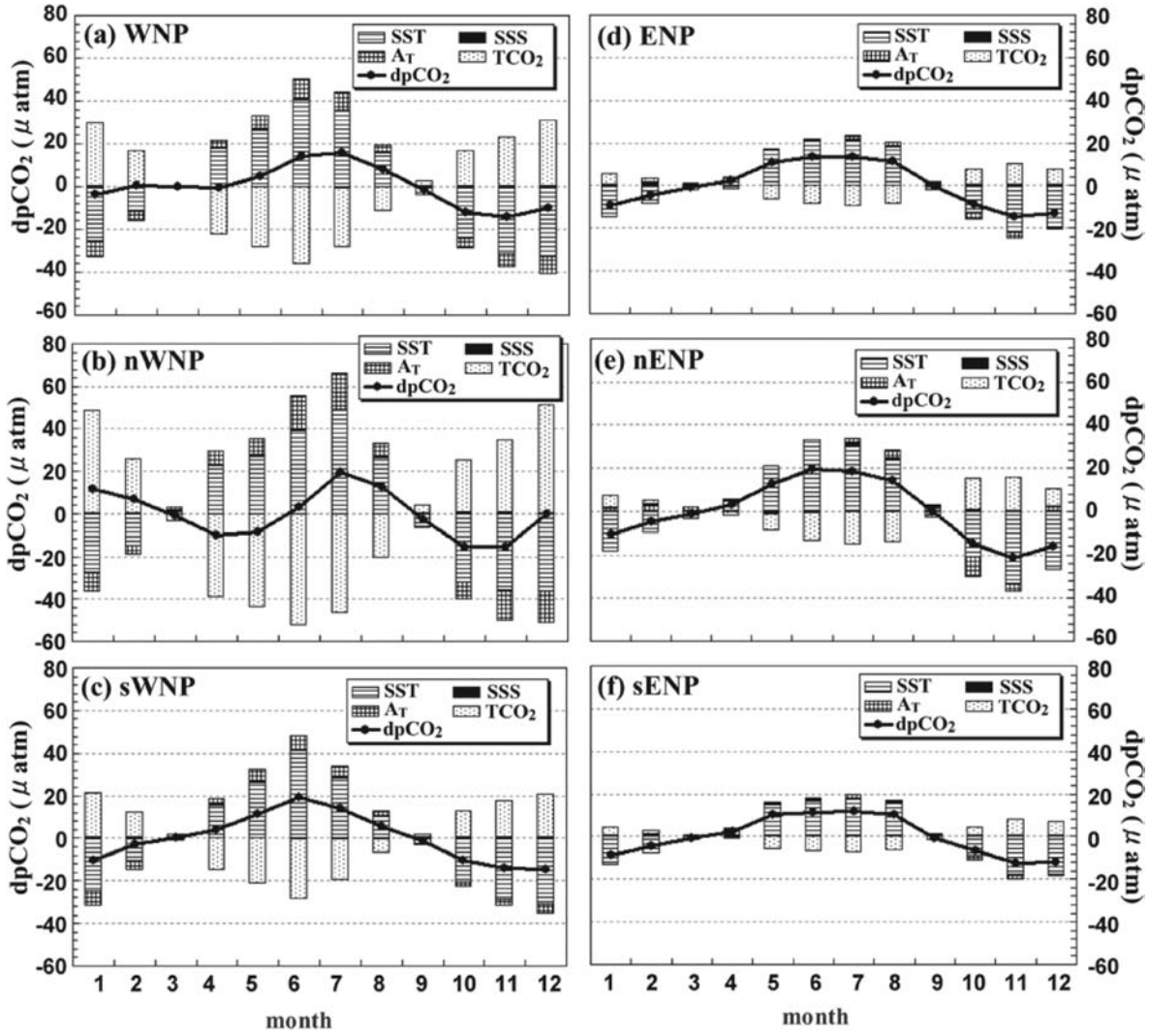


Fig. 5. Mean contributions of SST, SSS, A_T, and TCO_2 changes to the seasonal cycle of pCO_2^{sea} in the (a) entire WNP, (b) nENP (north of 35°N in the WNP), (c) sWNP (south of 35°N in the WNP), (d) entire ENP, (e) nENP (north of 35°N in the ENP), and (f) sENP (south of 35°N in the ENP) from 1999 to 2006. The change in the monthly pCO_2^{sea} between two successive months ($dpCO_2$) is shown in the latter month. The solid circles show the net change of the monthly mean pCO_2^{sea} between two months.

Eq. (2) again ($f(t) = \Delta pCO_2(t)$). Usually, the minimum ΔpCO_2 in the sWNP and ENP occurred in summer (August/September), and the maximum, in late winter (March) (Fig. 4c, d–f). In the nWNP, ΔpCO_2 showed two minima in summer (August/September) and late winter (February/March), and two maxima in late spring (May/June) and late fall (November/December) (Fig. 4b). In the sWNP, pCO_2^{sea} was slightly larger than pCO_2^{air} in summer, while, in the nWNP, pCO_2^{sea} was always lower than pCO_2^{air}. In the ENP, ΔpCO_2 was less than -20 μatm; hence, the ENP acts as a source of atmospheric CO_2 in summer.

During the annual cycle of ΔpCO_2, the peak-to-trough amplitude was larger in the ENP ($\sim$70 μatm) than in the WNP ($\sim$57 μatm). In the WNP, the peak-to-trough amplitude was large in the sWNP, while the opposite was found in the ENP (Fig. 4), suggesting a difference in the controlling factors between the two regions.

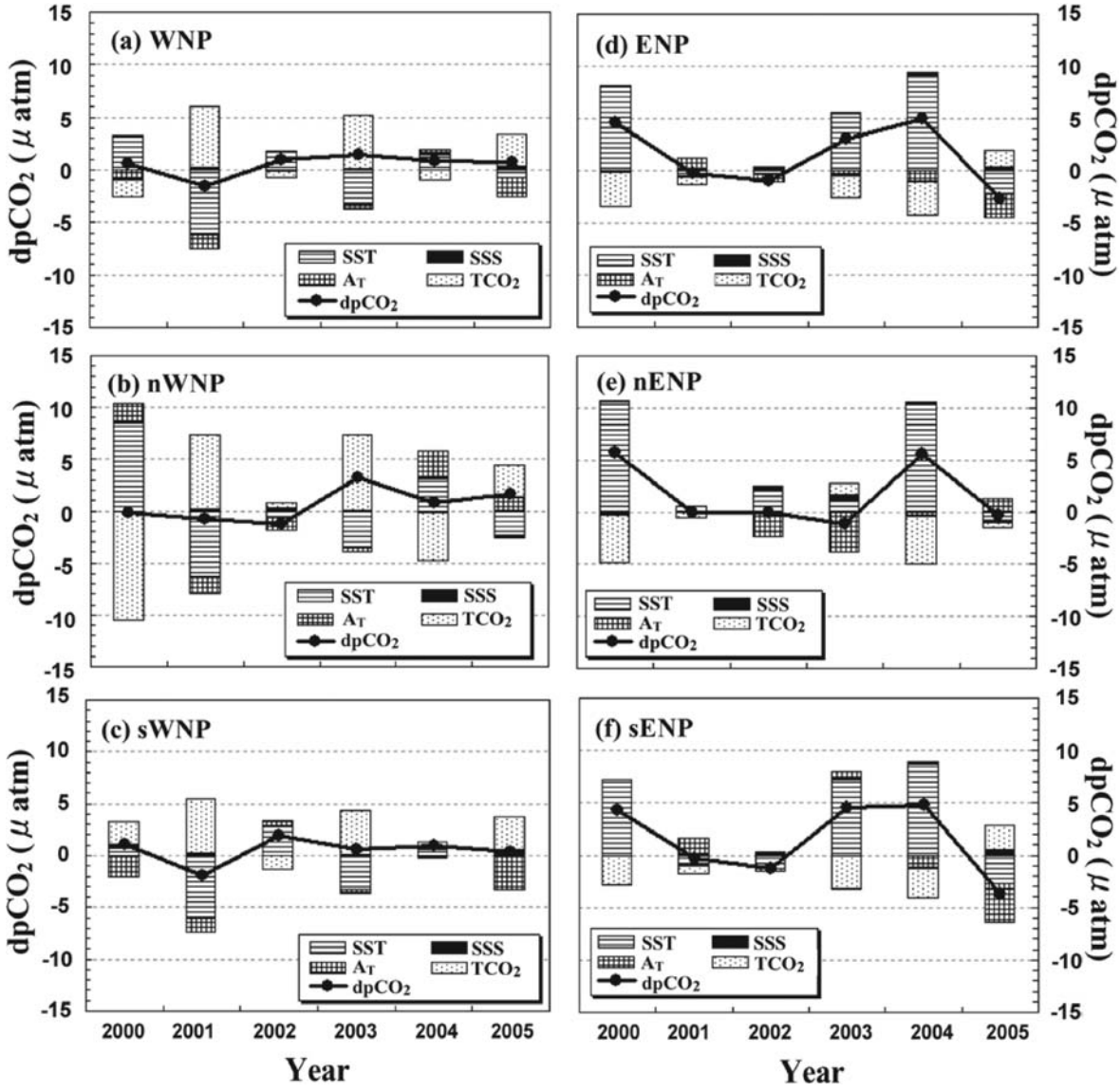


Fig. 6. The effect of SST, SSS, A_T, and TCO_2 changes in the interannual variation of pCO_2^{sea} in the (a) entire WNP, (b) nENP (north of 35°N in the WNP), (c) sWNP (south of 35°N in the WNP), (d) entire ENP, (e) nENP (north of 35°N in the ENP), and (f) sENP (south of 35°N in the ENP) from 1999 to 2006. The change in pCO_2^{sea} between two successive years ($dpCO_2$) is shown in the latter year. The solid circles show the net change of the annual mean pCO_2^{sea} between two years.

Due to the relatively small seasonal variability of pCO_2^{air}, the variation of ΔpCO_2 was mainly dependent on the pCO_2^{sea} variation. Therefore, to analyze the contribution of SST, SSS, A_T, and TCO_2 changes to the seasonal cycle of pCO_2^{sea}, we separated pCO_2^{sea} into differential terms (Takahashi *et al.* 1993):

$$\frac{dpCO_2^{sea}}{dt} = \frac{\partial pCO_2^{sea}}{\partial SST}\frac{dSST}{dt} + \frac{\partial pCO_2^{sea}}{\partial SSS}\frac{dSSS}{dt} + \frac{\partial pCO_2^{sea}}{\partial A_T}\frac{dA_T}{dt} + \frac{\partial pCO_2^{sea}}{\partial TCO_2}\frac{dTCO_2}{dt} \quad (3)$$

The first three terms of the right-hand side in Eq. (3) were computed using the thermodynamic

relationships described in DOE (1994). We used the dissociation constants for carbonic acids in seawater given by Roy *et al.* (1993). Residuals obtained by subtracting the sum of the first three terms of Eq. (3) from $(dpCO_2^{sea}/dt)$ were ascribed to the TCO_2 change via the air-sea CO_2 exchange, biological activity, and/or ocean dynamics.

Figure 5 illustrates the average contribution of each term in Eq. (3) from 1999 to 2006 to the change in the monthly pCO_2^{sea}. In both the WNP and ENP, the effect of SST varied in the same way as that of A_T and oppositely to that of TCO_2 during the annual cycle, thus damping the seasonal variation in pCO_2^{sea}. In the sWNP in June, the increase of pCO_2^{sea} with SST was estimated to be about 40 μatm, and the TCO_2 decrease was 30 μatm. The opposite occurred in December (Fig. 5c), when pCO_2^{sea} decreased by 35 μatm due to the SST decrease and increased by 20 μatm due to the TCO_2 increase. In the sWNP and ENP, the combined effect of SST, and A_T on pCO_2^{sea} is larger than that of TCO_2.

In the ENP, the magnitude of each effect on the seasonal variation in pCO_2^{sea} is small as compared with that in the sWNP. For example, pCO_2^{sea} increased by 17 μatm in June due to the SST rise and decreased by 18 μatm in November (Fig. 5d).

In the nWNP, the effects of both SST and TCO_2 varied largely as compared with those of sWNP (Fig. 5b), but the peak-to-trough amplitude of the seasonal variation in pCO_2^{sea} was slightly smaller than in the sWNP (Fig. 4). The effect of SST and A_T on pCO_2^{sea} was smaller than that of TCO_2 from January to May and larger from June to November. Thus, along with the negative dependence of A_T on pCO_2^{sea}, pCO_2^{sea} showed a maximum due to the effect of the TCO_2 increase in January, and due to the SST increase and A_T decrease in July. In general, in the subtropics, pCO_2^{sea} was at its maximum in summer due to the SST increase (thermodynamic temperature effect) and in the subarctic in winter due to the TCO_2 increase (mixed layer deepening and respiration). Therefore, the nWNP reveals a subtropical feature from summer to autumn and a subarctic one from winter to spring.

The thermodynamic salinity effect was fairly low in both the WNP and ENP. This implies that the great improvement in the regression analysis by introducing SSS as a variable was due to the expressivity of the ocean dynamics.

b. Interannual variation

Figure 6 shows the contributions of SST, SSS, A_T, and TCO_2 to the interannual variation of pCO_2^{sea}, which was calculated in the same way as the seasonal variation in pCO_2^{sea} (Section 3.2.a). In the WNP, both SST and TCO_2 are major factors for the interannual variation, and the effect of SST on pCO_2^{sea} was opposite to that of TCO_2 (Figs. 6a–c). In the ENP, the interannual variability of pCO_2^{sea} is much larger than that of WNP, which was mainly caused by the SST and the relatively small effect of TCO_2.

Table 2 shows increasing rates in pCO_2^{sea} in the WNP and ENP from 1999 to 2006. In the sWNP, pCO_2^{sea} increased at a rate of 0.48 ± 0.13 μatm yr^{-1}, and, in the nWNP, at a rate of 0.65 ± 0.17 μatm yr^{-1}; pCO_2^{sea} increased at a rate of 0.53 ± 0.11 μatm yr^{-1} for the entire WNP during the study period, a rate that is significantly slower than the atmospheric increase of 1.81 ± 0.01 μatm yr^{-1}. Consequently, ΔpCO_2 has increased at 1.28 ± 0.11 μatm yr^{-1} in the entire WNP, suggesting the possibility of increasing CO_2 uptake. In the western North Pacific (137°E), Inoue *et al.* (1995) and Midorikawa *et al.* (2006) reported a growth rate of wintertime pCO_2^{sea} which was nearly equal to that of air (1.6–1.8 μatm yr^{-1}). Increases of pCO_2^{sea} were mostly caused by the anthropogenic CO_2 uptake and, to a lesser amount, by the increase of SST. Takahashi *et al.* (2006) reported relatively low growth rates of pCO_2^{sea} (7.3–8.8 μatm $decade^{-1}$) in the western temperate zone (30–40°N, 150–180°E), which includes the Kuroshio extension. They discussed the effects of the outflow from the Sea of Okhotsk with a negative growth rate via the Oyashio Current and/or from the East China Sea with higher total alkalinity.

Table 2. Growth rate of pCO_2^{sea}, ΔpCO_2, and the air-sea CO_2 flux in the WNP and ENP.

	pCO_2^{sea} (μatm yr^{-1})	ΔpCO_2 (μatm yr^{-1})	CO_2 flux (mmol m^{-2} d^{-1} yr^{-1})
WNP	0.53 ± 0.11	1.28 ± 0.11	0.19 ± 0.05
nWNP*	0.65 ± 0.17	1.17 ± 0.17	0.26 ± 0.06
sWNP*	0.48 ± 0.13	1.34 ± 0.13	0.16 ± 0.05
ENP	1.32 ± 0.16	0.50 ± 0.16	0.09 ± 0.03
nENP*	1.13 ± 0.19	0.72 ± 0.23	0.18 ± 0.07
sENP*	1.39 ± 0.18	0.43 ± 0.18	0.05 ± 0.03

* nWNP and nENP indicate the regions north of 35°N, and sWNP and sENP indicate the regions south of 35°N.

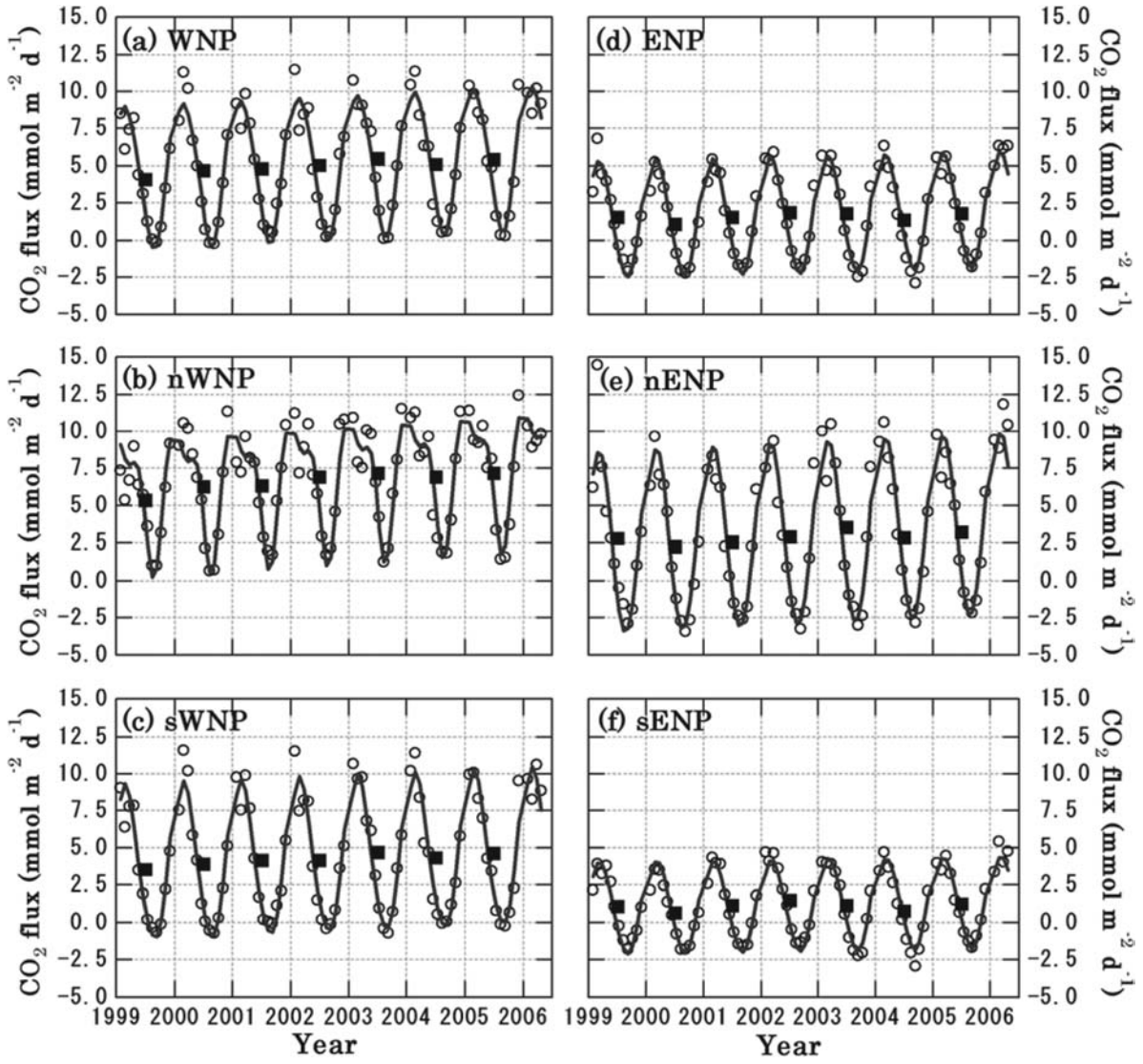


Fig. 7. Interannual variation in the air-sea CO_2 flux in the (a) entire WNP, (b) nENP (north of 35°N in the WNP), (c) sWNP (south of 35°N in the WNP), (d) entire ENP, (e) nENP (north of 35°N in the ENP), and (f) sENP (south of 35°N in the ENP) from 1999 to 2006. The open circle indicates the monthly air-sea CO_2 flux, and the solid squares indicate the annual mean value. The black line shows the results calculated using Eq. (2).

Midorikawa *et al.* (2009) examined the A_T change along 137°E over 1990s and reported an almost constant A_T, which may suggest the influence of the Sea of Okhotsk.

In the ENP, the annual average of pCO_2^{sea} increased at a rate of 1.32 ± 0.16 μatm yr^{-1}, which is nearly equal to that of Takahashi *et al.* (2006), who reported 15.4–17.1 μatm $decade^{-1}$ in the 30–40°N, 130–150°W. In Table 1, the linear time variation term in Eq. (1) gives the increase rate of pCO_2^{sea} at given SST and SSS. However, this coefficient itself is not a robust predictor of the long-term trend of pCO_2^{sea} in the WNP and ENP because year-to-year changes in SST and SSS could affect pCO_2^{sea}. For instance, at station ALOHA (22°45′N, 158°00′W), a large year-to-year increase in pCO_2^{sea} occurred along with SSS, which was caused by a reduction in rainfall (Dore *et al.* 2003)

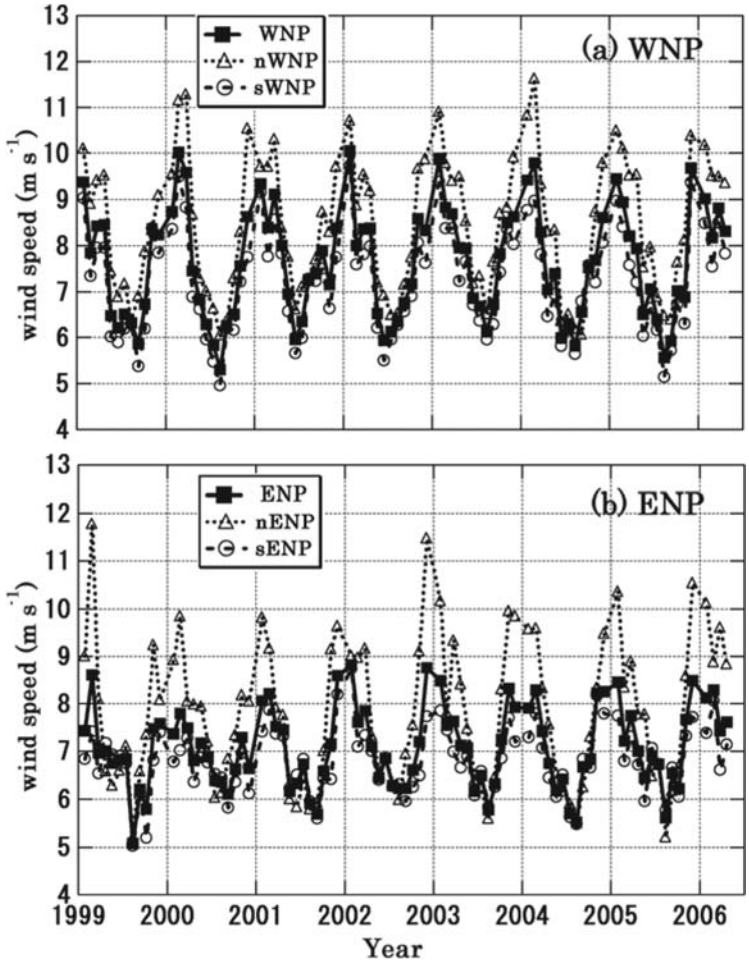


Fig. 8. Wind speed in the (a) WNP and (b) ENP from 1999 to 2006. The solid squares with a black line indicates the monthly average wind speed, the triangles with a dotted line represent the wind speed north of 35°N, and the open circle with a dashed line, show, the wind speed south of 35°N.

and the effect of a water mass exchange accompanied by a systematic large-scale shift of the North Pacific climate system (Keeling *et al.* 2004). The rate of increase of pCO_2^{sea}, that is, the linear time variation term in Eq. (1) (Table 1) multiplied by 12 deviates from the rate of increase at a fixed geographical position (Table 2), especially in the ENP, where the SST is a predominant factor for the interannual variation in pCO_2^{sea} (Figs. 6d–f).

3.3 Air-sea CO_2 flux

Figure 7 shows the variations in the air-sea CO_2 flux in the WNP and ENP from 1999 to 2006. In the WNP, the air-sea CO_2 flux was at its minimum within the range -0.2 to 0.6 mmol m^{-2} d^{-1} in August/September, following the ΔpCO_2 minimum, and at its maximum within the range 8.2 to 11.4 mmol m^{-2} d^{-1} in January/February, which is two or three months earlier than that of ΔpCO_2. The maximum air-sea CO_2 flux varied more significantly from year to year than the minimum flux. In winter, the air-sea CO_2 flux in the nWNP showed a different pattern from that of ΔpCO_2 (Figs. 4b, 7b) due to the relatively high wind speed (Fig. 8). In the ENP, the seasonal variation of the air-sea CO_2 flux was at its minimum within the range -2.9 to -1.8 mmol m^{-2} d^{-1} in August/September and at its maximum within the range 5.2 to 6.8 mmol m^{-2} d^{-1} in January/February (Fig. 7d), which is one or two months earlier than that of ΔpCO_2. The annual mean CO_2 uptake rate in the nWNP was generally more than 1.5 times that in

Table 3. Annual mean wind speed, ΔpCO_2, and the air-sea CO_2 flux in the WNP and ENP.

	year	Wind speed m s^{-1}	ΔpCO_2 μatm	Air-sea CO_2 flux mmol m^{-2} d^{-1}	error	Gt C yr^{-1}	error
WNP	1999	7.4	28.2	4.1	1.5	0.09	0.03
(5.0×10^6 km^2)	2000	7.4	29.4	4.7	1.5	0.10	0.03
	2001	7.7	32.8	4.8	1.6	0.11	0.03
	2002	7.5	33.7	5.0	1.6	0.11	0.03
	2003	7.9	34.1	5.5	1.7	0.12	0.04
	2004	7.5	35.0	5.1	1.6	0.11	0.03
	2005	7.5	36.0	5.4	1.5	0.12	0.03
nWNP	1999	8.2	34.8	5.4	1.8	0.03	0.01
(1.4×10^6 km^2)	2000	8.3	36.8	6.3	2.0	0.04	0.01
	2001	8.4	39.4	6.3	2.0	0.04	0.01
	2002	8.3	42.4	6.9	1.9	0.04	0.01
	2003	8.7	40.9	7.2	2.1	0.04	0.01
	2004	8.3	41.9	6.9	1.9	0.04	0.01
	2005	8.4	42.1	7.2	2.0	0.04	0.01
sWNP	1999	7.0	25.2	3.5	1.3	0.06	0.02
(3.6×10^6 km^2)	2000	7.0	26.0	3.9	1.3	0.06	0.02
	2001	7.3	29.8	4.1	1.4	0.07	0.02
	2002	7.2	29.7	4.1	1.4	0.07	0.02
	2003	7.5	30.9	4.7	1.5	0.07	0.02
	2004	7.2	31.8	4.3	1.4	0.07	0.02
	2005	7.0	33.2	4.6	1.3	0.07	0.02
ENP	1999	6.9	9.2	1.6	1.2	0.03	0.02
(4.4×10^6 km^2)	2000	6.9	6.4	1.1	1.2	0.02	0.02
	2001	7.0	8.4	1.5	1.3	0.03	0.02
	2002	7.2	11.2	1.9	1.3	0.04	0.03
	2003	7.2	10.0	1.8	1.3	0.03	0.03
	2004	7.0	6.8	1.4	1.3	0.03	0.02
	2005	7.1	11.3	1.8	1.3	0.03	0.03
nENP	1999	7.7	13.7	2.8	1.6	0.01	0.01
(1.0×10^6 km^2)	2000	7.7	9.8	2.3	1.6	0.01	0.01
	2001	7.5	11.7	2.6	1.5	0.01	0.01
	2002	7.9	13.5	2.9	1.7	0.01	0.01
	2003	8.0	16.5	3.6	1.7	0.02	0.01
	2004	7.6	12.8	2.9	1.5	0.01	0.01
	2005	7.8	14.9	3.3	1.6	0.01	0.01
sENP	1999	6.6	7.5	1.1	1.1	0.02	0.02
(3.4×10^6 km^2)	2000	6.6	5.1	0.7	1.1	0.01	0.02
	2001	6.8	7.2	1.1	1.2	0.02	0.02
	2002	6.9	10.3	1.5	1.2	0.02	0.02
	2003	6.9	7.5	1.1	1.2	0.02	0.02
	2004	6.8	4.5	0.8	1.2	0.01	0.02
	2005	6.8	10.0	1.3	1.2	0.02	0.02

the sWNP. In the ENP, the CO_2 uptake rate in the nENP was, on average, 2.8 times that in the sENP (Table 3).

Figure 9 shows the contribution of k_s, α, and ΔpCO_2 to the interannual variation of the air-sea CO_2 flux, which was calculated using Eq. (4):

$$\frac{dF}{dt} = \frac{\partial k_s}{\partial t}\alpha\Delta pCO_2 + k_s\frac{\partial \alpha}{\partial t}\Delta pCO_2 + k_s\alpha\frac{\partial \Delta pCO_2}{\partial t} \quad (4)$$

The effect of solubility on the interannual variation in the air-sea CO_2 flux was usually lower than 1%.

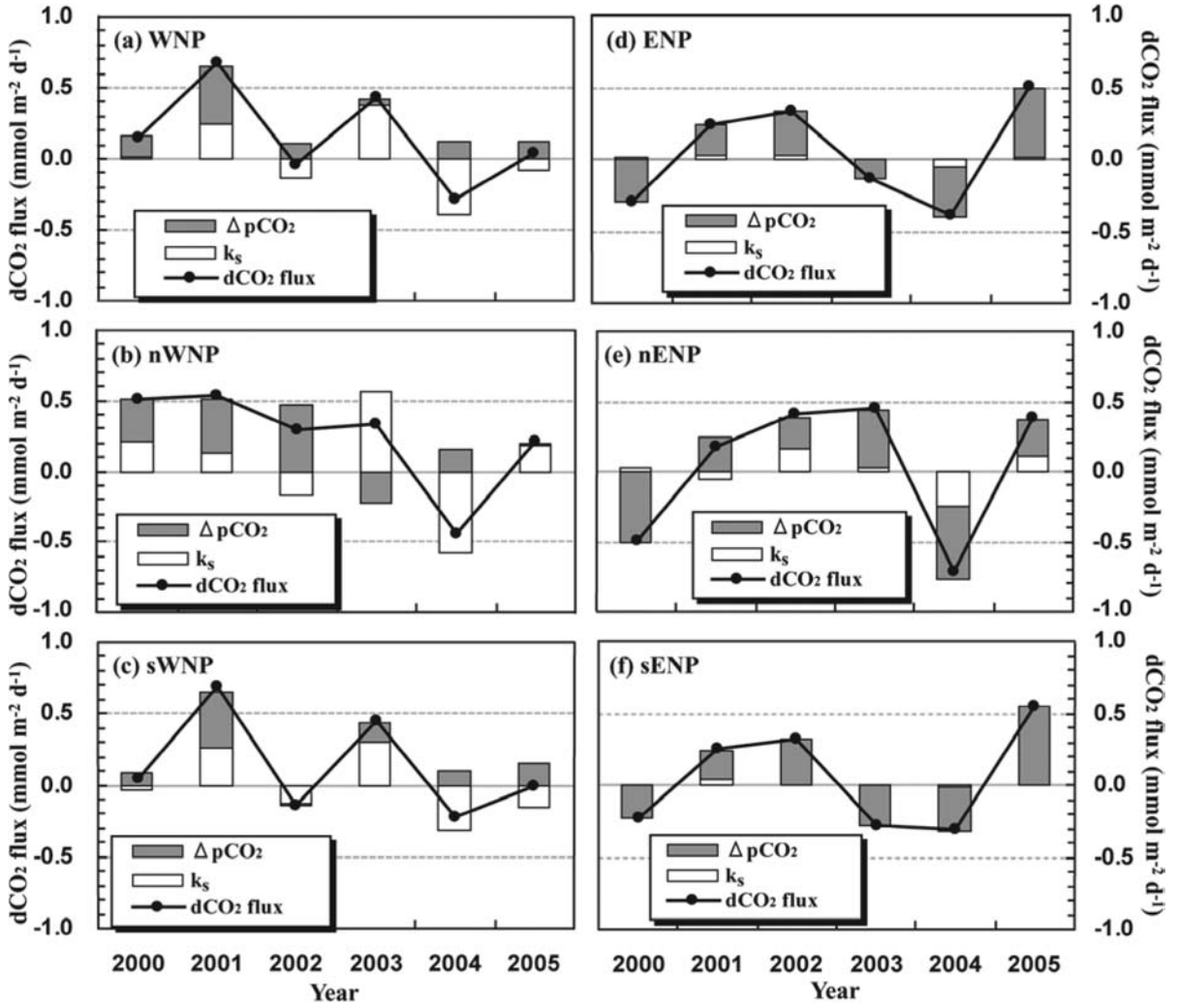


Fig. 9. Effect of the gas-transfer velocity (k_s) and ΔpCO_2 on the interannual variation in the air-sea CO_2 flux in the (a) WNP, (b) nENP, (c) sWNP, (d) entire ENP, (e) nENP, and (f) sENP from 1999 to 2006. The change in the air-sea CO_2 flux between two successive years (dCO_2 flux) is shown in the latter year. Because the effect of the CO_2 solubility on the interannual variation in the air-sea CO_2 flux was usually lower than 1% of the total, it is not shown here.

In the WNP, not only ΔpCO_2 but the gas-transfer velocity (wind speed) also plays an important role in determining the interannual variation in the air-sea CO_2 flux, whereas, in the ENP, ΔpCO_2 was the predominant factor.

From 1999 to 2006, the annual mean of the air-sea CO_2 flux increased at the rate of 0.19 ± 0.05 mmol m^{-2} d^{-1} yr^{-1} within the range 4.1 to 5.5 mmol m^{-2} d^{-1} in the WNP and at the rate of 0.09 ± 0.03 mmol m^{-2} d^{-1} yr^{-1} within the range 1.1 to 1.9 mmol m^{-2} d^{-1} in the ENP (Fig. 7 and Table 2). Although ΔpCO_2 in the sWNP increased at a rate similar to that the nWNP (Section 3.2.b), the air-sea CO_2 flux in the nWNP (0.26 ± 0.06 mmol m^{-2} d^{-1} yr^{-1}) increased more significantly than in the sWNP (0.16 ± 0.05 mmol m^{-2} d^{-1} yr^{-1}). In the sENP, the ΔpCO_2 increased at a rate of 0.43 ± 0.18 μatm yr^{-1}, and in the nENP, at a rate of 0.72 ± 0.23 μatm yr^{-1}. The air-sea CO_2 flux in the sENP increased at a rate of 0.05 ± 0.03 mmol m^{-2} d^{-1} yr^{-1}, and, in the nENP, at a rate of 0.18 ± 0.07 mmol m^{-2} d^{-1} yr^{-1}. In the nENP, the wind speed from 1999 to 2006 increased considerably, at a rate of 0.38 ± 0.19 m s^{-1} yr^{-1} in

December, 0.18 ± 0.06 m s^{-1} yr^{-1} in January, 0.18 ± 0.08 m s^{-1} yr^{-1} in March, and 0.18 ± 0.09 m s^{-1} yr^{-1} in April, when a relatively large ΔpCO_2 was seen. Therefore, the relatively large growth rate of the air-sea CO_2 flux in the nENP could be caused by the increase in wind speed.

In the ENP, the increase in the SST over the years and the changes in wind speed also indicate a possible link to the pattern of Pacific climate variability: Pacific Decadal Oscillation (PDO; Zhang *et al.* 1997; Mantua *et al.* 1997). The monthly PDO index, defined as the leading principal component of the North Pacific monthly SST variability, showed a negative phase starting in July 1998 and a turn to the positive phase in August 2002 (http://jisao.washington.edu/pdo/), from which we could expect increases in SST and wind speed during the observation period. Larger effects of PDO on the carbonate system can be expected in the eastern North Pacific, as observed in the correlation between the northeast Pacific marine ecosystem and the phase changes in PDO (Mantua *et al.* 1997). Long-term monitoring of the carbonate system is needed to gain an improved understanding of the variations in pCO_2^{sea} associated with PDO and global warming.

4. Summary

We investigated the seasonal and inter-annual variations of pCO_2^{sea} and the air-sea CO_2 flux in the western North Pacific (WNP; 25–40°N, 140–170°E) and eastern North Pacific (ENP; 25–40°N, 120–150°W) from 1999 to 2006 on the basis of the latest voluntary observation ship pCO_2^{sea} data.

In the WNP and ENP, the pCO_2^{sea} maximum occurred in late summer, and the minimum occurred in late winter. We analyzed the relative contribution of SST, SSS, A_T, and TCO_2 changes to the seasonal cycle of pCO_2^{sea}. In the ENP, the effect of SST and A_T on pCO_2^{sea} is larger than that of TCO_2, while, in the WNP TCO_2 affects pCO_2^{sea} as much as SST.

From 1999 to 2006, pCO_2^{sea} increased at a rate of 0.53 ± 0.11 μatm yr^{-1} in the WNP and 1.32 ± 0.16 μatm yr^{-1} in the ENP. In addition to the anthropogenic CO_2 uptake, the growth rate of pCO_2^{sea} in the WNP could relate to changes in the carbonate system in the high latitudes and that in the ENP to changes in the SST and SSS fields. Over the same period, the air-sea CO_2 flux increased at a rate of 0.19 ± 0.05 mmol m^{-2} d^{-1} yr^{-1} in the WNP and 0.09 ± 0.03 mmol m^{-2} d^{-1} yr^{-1} in the ENP, which suggests that the WNP will be a stronger sink for atmospheric CO_2. In the ENP, increases in the air-sea CO_2 flux derived from variations in SST, SSS, and wind speed suggest a possible linkage to the pattern of Pacific climate variability, such as the Pacific Decadal Oscillation (PDO). At the moment, however, we do not know the details of how and to what extent the PDO regime shift affects the carbonate chemistry in the North Pacific.

In this study, we demonstrated that the effect of TCO_2 variation is a key factor controlling pCO_2^{sea} variation, especially in the WNP. For further understanding of the variations in pCO_2^{sea}, it is necessary to clarify the temporal and spatial variations in TCO_2. Thus, long-term monitoring of the carbonate system including the carbon isotope, which allows us to evaluate biogeochemical processes, is needed for improved understanding of variations in pCO_2^{sea} in the wide area of the North Pacific.

Acknowledgments

This research was supported in part by a Grant-in-Aid for Scientific Research, "Western Pacific Sea-air Interaction Study (W-PASS)," of the Ministry of Education, Culture, Sports, Science, and Technology of Japan (#19030001), and by funding obtained from the Ministry of Environment, Japan within the Eco-Frontier Fellowship Program. We would like to thank the Japan Meteorological Agency, M.O. Ship Management Co., Ltd., Mitsui O.S.K. lines, and Toyofuji Shipping Co., Ltd., for the atmospheric/oceanic pCO_2 observations. We are also grateful to the captain, officers, and crews of the M/S *Alligator Liberty* and M/S *Pyxis* for their superb support.

References

Bates, N. R., A. F. Michaels, and A. H. Knap, 1996: Seasonal and interannual variability of oceanic carbon dioxide species at the U. S. JGOFS Bermuda Atlantic Time-series Study (BATS) site, *Deep-Sea Res.*, **43**, 347–383.

Chierici, M., A. Fransson, and Y. Nojiri, 2006: Biogeochemical processes as drivers of surface fCO_2 in contrasting provinces in the subarctic North Pacific Ocean, *Global Biogeochem. Cycles*, **20**, GB1009, doi:10.1029/2004GB002356.

DOE, 1994: Handbook of methods for analysis of the various parameters of the carbon dioxide system in sea water, version, 2. Edited by A. G. Dickson and C. Goyet. ORNL/CDIAC-74.

Dore, J. E., R. Lukas, D. W. Sadler, and D. M. Karl, 2003: Climate-driven changes to the atmospheric CO_2 sink in the subtropical North Pacific Ocean, *Nature*, **424**, 754–757.

Inoue, H. Y., H. Matsueda, M. Ishii, K. Fushimi, M. Hirota, I. Asanuma, and Y. Takasugi, 1995: Long-term trend of the partial pressure of carbon dioxide (pCO_2) in surface waters of the western North Pacific, 1984–1993, *Tellus*, **47B**, 391–413.

Ishii, M., H. Y. Inoue, H. Matsueda, S. Saito, K. Fushimi, K. Nemoto, T. Yano, H. Nagai, and T. Midorikawa, 2001: Seasonal variation in total inorganic carbon and its controlling processes in surface waters of the western North Pacific subtropical gyre, *Mar. Chem.*, **75**, 17–32.

Kawai, H., 1972: Hydrography of the Kuroshio Extension, in Kroshio: its physical aspects, Edited by H. Stommel and K. Yoshida, University of Tokyo Press, Tokyo, 235–352.

Keeling, C. D., H. Brix, and N. Gruber, 2004: Seasonal and long-term dynamics of the upper ocean carbon cycle at Station ALOHA near Hawaii, *Global Biogeochem. Cycles*, **18**, GB4006, doi:10.1029/2004GB002227.

Landrum, L. L., R. H. Gammon, R. A. Feely, P. P. Murphy, K. C. Kelly, C. E. Cosca, and R. F. Weiss, 1996: North Pacific Ocean CO_2 disequilibrium for spring through summer, 1985–1989, *J. Geophys. Res.*, **101**, C12, 28539–28555.

Lee, K., R. Wanninkhof, T. Takahashi, S. C. Doney, and R. A. Feely, 1998: Low interannual variability in recent oceanic uptake of atmospheric carbon dioxide, *Nature*, **396**, 155–159.

Lee, K., L. T. Tong, F. J. Millero, C. L. Sabine, A. G. Dickson, C. Goyet, G-H. Park, R. Wanninkhof, R. A. Feely, and R. M. Key, 2006: Global relationships of total alkalinity with salinity and temperature in surface waters of the world's oceans, *Geophys. Res. Lett.*, **33**, L19605, doi:10.1029/2006GL027207.

Mantua, N. J., S. R. Hare, Y. Zhang, J. M. Wallace, and R. C. Francis, 1997: A Pacific interdecadal climate oscillation with impacts on salmon production, *Bull. Amer. Meteor. Soc.*, **78**, 1069–1079.

Roy, R. N., L. N. Roy, K. M. Vogel, C. P. Moore, T. Pearson, C. E. Good, F. J. Millero, and D. J. Cambell, 1993: Determination of the ionization constants of carbonic acid in seawater. *Mar. Chem.*, **44**, 249–268.

Midorikawa, T., K. Ogawa, H. Kamiya, N. Hiraishi, T. Umeda, A. Wada, K. Nemoto, and M. Ishii, 2003: Interannual variations of net community production and air-sea CO_2 flux from winter to spring in the western subarctic North Pacific, *Tellus*, **55B**, 466–477.

Midorikawa, T., M. Ishii, K. Nemoto, H. Kamiya, A. Nakadate, S. Masuda, H. Matsueda, T. Nakano, and H. Y. Inoue, 2006: Interannual variability of winter oceanic CO_2 and sea-air CO_2 flux in the western North Pacific for 2 decades, *J. Geophys. Res.*, **111**, C07S02, doi:10.1029/2005JC003095.

Midorikawa, T., M. Ishii, D. Sasano, N. Kosugi, T. Motoi, H. Kamiya, A. Nakadate, and H. Y. Inoue, 2009: Estimation of long-term trend of pH based on the variations of carbonate parameters observed in the western North Pacific, ICDC8, Jena, Sept 13–19.

Ogawa, K., et al., 2006: Shipboard measurements of atmospheric and surface seawater pCO_2 in the North Pacific carried out from January 1999 to October 2000 on the voluntary observation ship MS Alligator Liberty, *Pap. Meteor. Geophys.*, **57**, 37–46, doi:10.2467/mripapers.57.37.

Polovina, J. J., E. Howell, D. R. Kobayashi, and M. P. Seki, 2001: The transition zone chlorophyll front, a dynamic global feature defining migration and forage habitat for marine resources, *Prog. Oceanogr.*, **49**, 469–483.

Rodgers, K. B., J. L. Sarmiento, O. Aumont, C. Crevoiser, C. de Boyer Montégut, and N. Metzl, 2008: A wintertime uptake window for anthropogenic CO_2 in the North Pacific, *Global Biogeochem. Cycles*, **22**, GB2020, doi:10.1029/2006GB002920.

Sabine, C., et al., 2004: The oceanic sink for anthropogenic CO_2, *Science*, **305**, 367–371.

Stephens, M. P., G. Samuels, D. B. Olson, R. A. Fine, and T. Takahashi, 1995: Sea-air flux of CO_2 in the North Pacific using shipboard and satellite data, *J. Geophys. Res.*, **100**, C7, 13571–13583.

Suga, T., and K. Hanawa, 1990: The mixed layer climatology in the northwestern part of the North Pacific subtropical gyre and the formation area of Subtropical Mode Water, *J. Mar. Res.*, **48**, 543–566.

Sweeney, C., E. E. Gloor, A. R. Jacobson, R. M. Key, G. McKinly, J. L. Sarmiento, and R. Wanninkhof, 2007: Constraining global air-sea gas exchange for CO_2 with recent bomb ^{14}C measurements, *Global Biogeochem. Cycles*, **21**, doi:10.1029/2006GB002784.

Takahashi, T., J. Olafsson, J. G. Goddard, D. W. Chipman, and S. C. Sutherland, 1993: Seasonal variation of CO_2 and nutrients in the high-latitude surface oceans: A comparative study, *Global Biogeochem. Cycles*, **14**, 1267–1281.

Takahashi, T., R. A. Feely, R. F. Weiss, R. H. Wanninkhof, D. W. Chipman, S. C. Sutherland, and T. T. Takahashi, 1997: Global air-sea flux of CO_2: An estimate based on measurements of sea-air pCO_2 difference, *Proc. Natl. Acad. Sci.*, USA, **94**, 8292–8299.

Takahashi, T., S. C. Sutherland, R. A. Feely, and R. Wanninkhof, 2006: Decadal change of the surface water pCO_2 in the North Pacific: A synthesis of

35 years of observations, *J. Geophys. Res.*, **111**, C07S05, doi:10.1029/2005JC003074.

Takahashi et al., 2009: Climatological mean and decadal change in surface ocean pCO_2, and net sea-air CO_2 flux over the global oceans, *Deep-Sea Res.* II, **56**, 554–577.

Tans, P. P., I. Y. Fung, and T. Takahashi, 1990: Observational constraints on the global atmospheric CO_2 budget, *Science*, **247**, 1431–1438.

Wanninkhof, R., 1992: Relationship between wind speed and gas exchange over the ocean, *J. Geophys. Res.*, **97**, 7373–7382.

Wanninkhof, R., R. A. Feely, H. Chen, C. Cosca, and P. P. Murphy, 1996: Surface water fCO_2 in the eastern equatorial Pacific during the 1992–1993 El Niño, *J. Geophys. Res.*, **101**, 16,333–16,343.

Weiss, R. F., 1974: Carbon dioxide in water and seawater: The solubility of a non-ideal gas, *Mar. Chem.*, **2**, 203–215.

Weiss, R. F., R. A. Jahnke, and C. D. Keeling, 1982: Seasonal effects of temperature and salinity on the partial pressure of CO_2 in seawater, *Nature*, **300**, 511–513.

Wooster, W. S., and J. L. Reid, Jr., 1963: Eastern boundary currents, in The Sea, edited by M. N. Hill, *Wiley Interscience*, NY, 253–280.

Zeng, J., Y. Nojiri, P. P. Murphy, C. S. Wong, and Y. Fujinuma, 2002: A comparison of ΔpCO_2 distributions in the northern North Pacific using results from a commercial vessel in 1995–1999, *Deep-Sea Res.*, **49**, 5303–5315.

Zhang, Y., J. M. Wallace, and D. S. Battisti, 1997: ENSO-like interdecadal variability: 1900–93, *J. Climate*, **10**, 1004–1020.